



King Saud University  
Arabian Journal of Chemistry

[www.ksu.edu.sa](http://www.ksu.edu.sa)  
[www.sciencedirect.com](http://www.sciencedirect.com)



## ORIGINAL ARTICLE

# Metal complexes of azo compounds derived from 4-acetamidophenol and substituted aniline

S.M. Abdallah \*

Workers University, Aswan, Egypt

Received 20 July 2010; accepted 28 August 2010

Available online 7 September 2010

## KEYWORDS

Azo compounds;  
Metal complexes;  
Spectroscopy;  
Thermal analysis;  
Biological activity

**Abstract** The Ni(II) and Cu(II) complexes of four azo compounds ( $H_2L^{1-4}$ ), namely, 2-(p-X-phenylazo)-4-acetamidophenol (X = OCH<sub>3</sub>, NO<sub>2</sub>, Br, and H for  $H_2L^1$ ,  $H_2L^2$ ,  $H_2L^3$ , and  $H_2L^4$ , respectively) were prepared and characterized on the basis of their analytical, spectroscopic, magnetic, and conductance data. The isolated complexes are found to have the general formulae  $[M(HL^{1-4})Cl(H_2O)_3]$  (M = Ni(II) and Cu(II)). The chelates are found to have octahedral structure. The infrared spectra show that  $H_2L^{1-4}$  ligands are coordinated to the metal ions in a uninegative bidentate manner, with NO donor sites of the azo N and the deprotonated phenolic O. The ligands and their chelates are subjected to thermal analysis. The biological activity of the synthesized ligands and their metal complexes also are screened against the adult *Tribolium confusum* mortality. They showed remarkable biological activity.

© 2010 King Saud University. Production and hosting by Elsevier B.V. All rights reserved.

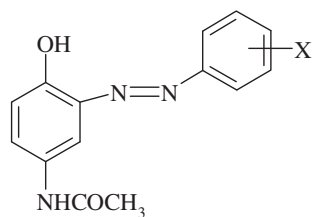
## 1. Introduction

Azo compounds are highly coloured that enjoy widespread use as dyes and pigments in a variety of applications that include textile dyeing (Koh and Greaves, 2001) as well as non-linear and photoelectronics (Katz et al., 1987), especially in optical

information storage (Wang et al., 2000; Li et al., 2009; Gan et al., 2000; Sabi et al., 2003). Azo compounds are very important molecules and have attracted much attention in both academic and applied research (Zollinger, 1961, 1987; Nishihara, 2004). For example, azo derivatives and their metal complexes are very important pigments for synthetic leather and vinyl polymers. On the other hand, azo compounds are known to be involved in a number of biological reactions, such as inhibition of DNA, RNA, and protein synthesis, nitrogen fixation, and carcinogenesis (Badea et al., 2004). Furthermore, high-density optical data storage has been a subject of extensive research in the past decade. In general, cyanine dyes, phthalocyanine dyes, and metal–azo complex dyes are used in the recording layer of DVD-R (Digital Versatile Disc-Recordable) discs. It has been reported that the new technology, which employs 405 nm blue–violet diode lasers, requires a new optical-recording medium matching the 405 nm wavelength laser. In comparison with the dyes them-

\* Tel.: +002 0110900667; fax: +00202 35728843.  
E-mail address: [Sayed\\_Abdallah2010@yahoo.com](mailto:Sayed_Abdallah2010@yahoo.com)





$H_2L^1$ ; X = OCH<sub>3</sub>

$H_2L^2$ ; X = p-NO<sub>2</sub>

$H_2L^3$ ; X = p-Br

$H_2L^4$ ; X = H

**Figure 1** Structures of azo ligands ( $H_2L^{1-4}$ ).

selves, metal-azo dyes are more light stable, allow for easier control of the wavelength by selection of the appropriate substituent groups, and have good thermal stability (Geng et al., 2004; Bin et al., 2003; Fu-Xin et al., 2003; Hamada et al., 1997; Suzuki et al., 1999; Nejati et al., 2009; Li et al., 2010). Because of the good thermal stability of azo compounds and the ease with which the absorption band may be tuned by varying the substituents, one of the many applications of azo compounds is in optical data storage. In a continuation to the interest in the synthesis of azo-based compounds (Mohamed et al., 2001a,b, 2002), the present work aimed chiefly to throw more light on the characterization of Ni(II) and Cu(II) complexes of four azo compounds. The coordination behaviour of these azo compounds towards Ni(II) and Cu(II) ions is reported using different analytical tools. The structures of the azo ligands under investigation are given in Fig. 1.

## 2. Experimental

### 2.1. Materials and methods

All chemicals used were of the analytical reagent grade. They included 4-acetamidophenol (Sigma), aniline, 4-methoxyaniline, 4-nitroaniline and 4-bromoaniline (Aldrich), sodium nitrite and hydroxide (BDH), ethyl alcohol (Adwic), and the

disodium salt of ethylenediaminetetraacetic acid (Adwic).  $CuCl_2 \cdot 2H_2O$  (Prolabo) and  $NiCl_2 \cdot 6H_2O$  (BDH) were used as received. The elemental analyses (C, H, and N) were made at the Microanalytical Center at Cairo University. IR spectra were recorded on a Perkin-Elmer FT-IR type 1650 spectrophotometer. The solid reflectance spectra were measured on a Shimadzu 3101 PC spectrophotometer. The molar magnetic susceptibilities were measured on powdered samples using the Faraday method. The conductance measurements were carried out using a Sybron-Barnstead conductometer. Shimadzu TG-50H and DTA-50H thermal analyzers were used to record simultaneously TG, DTG, and DTA curves. The experiments were carried out in dynamic nitrogen atmosphere ( $20 \text{ ml min}^{-1}$ ) with a heating rate of  $10 \text{ }^\circ\text{C min}^{-1}$  in the temperature range of 20–1000  $^\circ\text{C}$  using platinum crucibles. Metal contents were determined by titration against standard EDTA after complete decomposition of the complexes with aqua regia in a Kjeldahl flask several times.

### 2.2. Synthesis of azo ligands ( $HL^{1-4}$ ) (Mohamed, 1996)

p-X-Aminobenzene (0.93, 1.72, 1.23, and 1.38 g for X = p-H, -Br, -OMe, and -NO<sub>2</sub>, respectively, 10 mmol) was mixed with HCl (11.5 M, 5 ml) and diazotized below 5  $^\circ\text{C}$  with NaNO<sub>2</sub> (2.07 g, 10 mmol). The resulting diazonium chloride was coupled with an alcoholic NaOH (3 g, 25 ml) solution of 4-acetamidophenol (4.53 g, 10 mmol) below 5  $^\circ\text{C}$ . The product was separated by filtration, purified by crystallization from diethyl ether and dried in vacuo over anhydrous calcium chloride. The red azo products are produced in 69–78% yield.

### 2.3. Synthesis of the complexes

The appropriate metal chloride (Cu(II) and Ni(II) ions) (10 mmol) in ethanol-water (1:1) (25 mL) mixture was added to the solution of the azo compound (0.40 g, 10 mmol) in the same solvent mixture (50 mL). The resulting solution was stirred under reflux for 0.5 h whereupon the complexes were precipitated. They were removed by filtration, washed with 1:1 ethanol/water and with Et<sub>2</sub>O.

**Table 1** Analytical and physical data of  $H_2L^{1-4}$  ligands and their complexes.

Compound	Colour (% yield)	M.P. ( $^\circ\text{C}$ )	% Found (calcd.)					$\mu_{\text{eff.}}$ (B.M.)
			C	H	N	Cl	M	
$[Cu(HL^1)Cl(H_2O)_3] \cdot 1.5H_2O$	Brown	> 300	38.33	4.48	9.42	7.96	14.00	1.95
$C_{15}H_{23}ClCuN_3O_{7.5}$	(75)		(38.79)	(4.96)	(9.05)	(7.65)	(13.64)	
$[Ni(HL^1)Cl(H_2O)_3]$	Brown	> 300	41.14	4.45	9.55	7.91	13.91	3.95
$C_{15}H_{20}ClNiN_3O_6$	(73)		(41.62)	(4.62)	(9.71)	(8.21)	(13.64)	
$[Cu(HL^2)Cl(H_2O)_3]$	Brown	> 300	37.40	3.51	12.58	7.32	14.44	1.91
$C_{14}H_{17}ClCuN_4O_7$	(70)		(37.09)	(3.97)	(12.36)	(7.83)	(14.02)	
$[Ni(HL^2)Cl(H_2O)_3] \cdot 2H_2O$	Brown	> 300	34.23	4.36	12.08	7.12	12.56	3.85
$C_{14}H_{21}ClNiN_4O_9$	(78)		(34.75)	(4.34)	(11.58)	(7.34)	(12.20)	
$[Cu(HL^3)Cl(H_2O)_3]$	Brown	> 300	34.83	3.57	8.22	7.68	13.52	1.92
$C_{14}H_{17}BrClCuN_3O_5$	(69)		(34.57)	(3.50)	(8.64)	(7.30)	(13.07)	
$[Ni(HL^3)Cl(H_2O)_3]$	Brown	> 300	34.51	3.75	8.20	6.98	12.60	3.90
$C_{14}H_{17}BrClNiN_3O_5$	(72)		(34.89)	(3.53)	(8.72)	(7.37)	(12.25)	
$[Cu(HL^4)Cl(H_2O)_3]$	Brown	> 300	41.38	3.92	9.96	8.42	15.16	2.02
$C_{14}H_{18}ClCuN_3O_5$	(77)		(41.28)	(4.42)	(10.32)	(8.72)	(15.60)	
$[Ni(HL^4)Cl(H_2O)_3]$	Brown	> 300	41.11	4.60	10.10	8.42	14.32	3.88
$C_{14}H_{18}ClNiN_3O_5$	(70)		(41.84)	(4.48)	(10.46)	(8.84)	(14.69)	

**Table 2** IR spectral data (4000–400 cm<sup>-1</sup>) of H<sub>2</sub>L<sup>1-4</sup> ligands and their complexes.

Compound	$\nu(\text{OH})$	$\nu(\text{N}=\text{N})$	$\nu(\text{C}-\text{O})$	$\nu(\text{M}-\text{O})$	$\nu(\text{M}-\text{N})$
H <sub>2</sub> L <sup>1</sup>	3291br	1509m	1247m	–	–
[Cu(HL <sup>1</sup> )Cl(H <sub>2</sub> O) <sub>3</sub> ].1.5H <sub>2</sub> O	3337br	1511sh	1251sh	572s	529s
[Ni(HL <sup>1</sup> )Cl(H <sub>2</sub> O) <sub>3</sub> ]	3375br	1510sh	1249sh	530s	500w
H <sub>2</sub> L <sup>2</sup>	3321br	1519sh	1278s	–	–
[Cu(HL <sup>2</sup> )Cl(H <sub>2</sub> O) <sub>3</sub> ]	3381br	1517m	1275s	559s	524s
[Ni(HL <sup>2</sup> )Cl(H <sub>2</sub> O) <sub>3</sub> ].2H <sub>2</sub> O	3284br	1518sh	1279s	550w	524s
H <sub>2</sub> L <sup>3</sup>	3285br	1483m	1271m	–	–
[Cu(HL <sup>3</sup> )Cl(H <sub>2</sub> O) <sub>3</sub> ]	3331br	1484sh	1275m	539w	519s
[Ni(HL <sup>3</sup> )Cl(H <sub>2</sub> O) <sub>3</sub> ]	3377br	1482s	1273s	560w	522s
H <sub>2</sub> L <sup>4</sup>	3284br	1492m	1270m	–	–
[Cu(HL <sup>4</sup> )Cl(H <sub>2</sub> O) <sub>3</sub> ]	3340br	1490sh	1275s	548w	524w
[Ni(HL <sup>4</sup> )Cl(H <sub>2</sub> O) <sub>3</sub> ]	3386br	1493m	1272s	560w	520s

Sh = sharp, m = medium, br = broad, s = small, w = weak.

### 3. Results and discussion

The results of elemental analyses are in good agreement with those required by the proposed formulae given in Table 1.

#### 3.1. IR spectra and mode of bonding

As mentioned, the ligands have different coordinating sites. The IR has proven to be, in this particular case, a suitable technique to give enough information to elucidate the way of bonding of the ligands. Thus a detailed interpretation of IR spectra of these and the effect of binding of Ni(II) and Cu(II) ions on the vibration frequencies of the free ligands are discussed in this paper. The IR spectra of the free ligands and their metal complexes are carried out in the 4000–200 cm<sup>-1</sup> range (Table 2).

The IR spectra show broad-stretching vibration bands at 3284, 3321, 3285, and 3284 cm<sup>-1</sup> for H<sub>2</sub>L<sup>1</sup>, H<sub>2</sub>L<sup>2</sup>, H<sub>2</sub>L<sup>3</sup>, and H<sub>2</sub>L<sup>4</sup>, respectively, which could be attributed to OH of the phenolic group. The presence of coordinated water molecules renders it difficult to confirm the participation of the phenolic OH group in chelate formation. The bands observed at 1247, 1278, 1271, and 1270 cm<sup>-1</sup> are attributed to the  $\nu(\text{C}-\text{O})$  stretching vibration of the phenolic group for H<sub>2</sub>L<sup>1</sup>, H<sub>2</sub>L<sup>2</sup>, H<sub>2</sub>L<sup>3</sup>, and H<sub>2</sub>L<sup>4</sup>, respectively. These bands are shifted to higher or lower frequencies in all the complexes indicating coordination through the deprotonated phenolic OH group (Mohamed et al., 2001a,b, 2002). The strong bands observed at 1509, 1519, 1483, and 1492 cm<sup>-1</sup> in the spectra of the H<sub>2</sub>L<sup>1</sup>, H<sub>2</sub>L<sup>2</sup>, H<sub>2</sub>L<sup>3</sup>, and H<sub>2</sub>L<sup>4</sup>, respectively, may be attributed to  $\nu(\text{N}=\text{N})$  which shifted to higher or lower frequencies in all the complexes, indicating its involvement in the coordination of the ligands to the metal ions (Mohamed et al., 2001a,b, 2002). In the far IR spectra of all the complexes, there are new bands observed in the region of 580–400 cm<sup>-1</sup> which are absent in the spectrum of the free ligand. The bands observed at 500–529 cm<sup>-1</sup> (M–N) and 530–572 cm<sup>-1</sup> (M–O) (Table 2) provide conclusive evidence concerning the bonding of nitrogen and oxygen to the metal ions (Zaki et al., 1998). Therefore, the IR spectra indicate that the ligands coordinate through the deprotonated phenolic O and azo N.

#### 3.2. Electronic spectra measurements

As further structural tools, solid reflectance spectral studies have been used to confirm the geometry of the complexes.

The diffused reflectance spectra of the Ni(II) complexes display three bands at  $\nu_1$ : 14,771–15,625 cm<sup>-1</sup>:  ${}^3\text{A}_{2g} \rightarrow {}^3\text{T}_{2g}$ ;  $\nu_2$ : 17,361–18,484 cm<sup>-1</sup>:  ${}^3\text{A}_{2g} \rightarrow {}^3\text{T}_{1g}(\text{F})$ , and  $\nu_3$ : 20,704–21,978 cm<sup>-1</sup>:  ${}^3\text{A}_{2g} \rightarrow {}^3\text{T}_{1g}(\text{P})$  indicating octahedral configuration of the chelates (Mohamed et al., 2001a,b; Mohamed, 1996; Cotton et al., 1999). The spectra show also bands at 25,227–26,465 cm<sup>-1</sup> which may be attributed to ligand and to metal charge transfer.

The reflectance spectra of the Cu(II) complexes consist of low intensity shoulder bands centered at 14,286–14,970 and 17,241–17,391 cm<sup>-1</sup> (Mohamed et al., 2001a,b; Mohamed, 1996; Cotton et al., 1999), indicating the existence of the Cu(II) complexes in octahedral geometry.

The observed magnetic moment value of the Cu(II) and Ni(II) complexes are listed in Table 1 and the obtained values confirm the octahedral geometry.

#### 3.3. Thermal analyses (TG and DTG) studies

Table 3 shows the TG and DTG results of thermal decomposition of the metal chelates. The thermograms of the [Ni(HL<sup>1</sup>)Cl(H<sub>2</sub>O)<sub>3</sub>], [Cu(HL<sup>4</sup>)Cl(H<sub>2</sub>O)<sub>4</sub>], and [Ni(HL<sup>4</sup>)Cl(H<sub>2</sub>O)<sub>3</sub>] chelates show four decomposition steps within the temperature range of 50 to 1000, 30 to 900, and 30 to 900 °C, respectively. The first step of decomposition within the temperature range of 50–230, 30–120, and 30–900 °C occurred with the loss of two water molecules and HCl, HCl, and HCl gases with an estimated mass loss of 16.29% (16.76), 7.26% (8.99%), and 10.68% (calcd. 9.09%) for [Ni(HL<sup>1</sup>)Cl(H<sub>2</sub>O)<sub>3</sub>], [Cu(HL<sup>4</sup>)Cl(H<sub>2</sub>O)<sub>4</sub>], and [Ni(HL<sup>4</sup>)Cl(H<sub>2</sub>O)<sub>3</sub>] chelates, respectively. The remaining three steps of decomposition take place in the temperature range of 230 to 1000, 120 to 900, and 100 to 900 °C which are attributed to the loss of HL<sup>1</sup>, two water molecules and HL<sup>4</sup> and two water molecules and HL<sup>4</sup> for [Ni(HL<sup>1</sup>)Cl(H<sub>2</sub>O)<sub>3</sub>], [Cu(HL<sup>4</sup>)Cl(H<sub>2</sub>O)<sub>4</sub>], and [Ni(HL<sup>4</sup>)Cl(H<sub>2</sub>O)<sub>3</sub>] chelates, respectively.

It is obvious that, [Cu(HL<sup>1</sup>)Cl(H<sub>2</sub>O)<sub>3</sub>].1.5H<sub>2</sub>O and [Ni(HL<sup>2</sup>)Cl(H<sub>2</sub>O)<sub>3</sub>].2H<sub>2</sub>O chelates show five steps of decomposition. The first step of decomposition within the temperature

**Table 3** Thermoanalytical results (TG and DTG) of metal complexes.

Compound	TG range (°C)	DTG <sub>max</sub> (°C)	n*	Estim. (calcd) %		Assignment	Metallic residue
				Mass loss	Total mass loss		
[Cu(HL <sup>1</sup> )Cl(H <sub>2</sub> O) <sub>3</sub> ].1.5H <sub>2</sub> O	25–130	55, 145, 268, 545, 816	1	6.22 (5.82)		Loss of 1.5H <sub>2</sub> O	CuO
	130–330		2	16.35 (15.63)		Loss of HCl and 2H <sub>2</sub> O	
	330–900		2	61.16 (61.21)	83.73 (82.66)	Loss of L <sup>1</sup>	
[Ni(HL <sup>1</sup> )Cl(H <sub>2</sub> O) <sub>3</sub> ]	50–230	151, 269, 409, 851	1	16.29 (16.76)		Loss of 2H <sub>2</sub> O and HCl	NiO
	230–1000		3	65.37 (66.13)	81.66 (82.89)	Loss of HL <sup>1</sup>	
[Cu(HL <sup>2</sup> )Cl(H <sub>2</sub> O) <sub>3</sub> ]	30–100	64, 153, 261, 377, 550	1	8.06 (8.08)		Loss of HCl	CuO
	100–190		1	742 (7.96)		Loss of 2H <sub>2</sub> O	
	190–800		3	67.81 (66.59)	83.29 (82.63)	Loss of H <sub>2</sub> L <sup>2</sup>	
[Ni(HL <sup>2</sup> )Cl(H <sub>2</sub> O) <sub>3</sub> ].2H <sub>2</sub> O	30–100	85, 181, 258, 341, 693	1	7.24 (7.45)		Loss of 2H <sub>2</sub> O	NiO
	100–300		2	18.49 (18.72)		Loss of 3H <sub>2</sub> O and HCl	
	300–900		2	57.17 (58.74)	82.90 (84.91)	Loss of L <sup>2</sup>	
[Cu(HL <sup>3</sup> )Cl(H <sub>2</sub> O) <sub>3</sub> ]	30–120	83, 147, 257, 822	1	8.51 (7.54)		Loss of HCl	CuO
	120–250		1	12.47 (11.52)		Loss of 3H <sub>2</sub> O	
	250–950		2	64.54 (65.50)	85.52 (84.56)	Loss of HL <sup>3</sup>	
[Ni(HL <sup>3</sup> )Cl(H <sub>2</sub> O) <sub>3</sub> ]	30–100	51, 162, 519, 592, 796	1	7.17 (7.58)		Loss of HCl	NiO
	100–350		1	24.65 (24.30)		Loss of 2H <sub>2</sub> O and HBr	
	350–850		3	57.34 (57.11)	89.16 (88.99)	Loss of C <sub>14</sub> H <sub>17</sub> N <sub>3</sub> O <sub>3</sub>	
[Cu(HL <sup>4</sup> )Cl(H <sub>2</sub> O) <sub>3</sub> ]	30–120	81, 182, 634, 822	1	7.26 (8.99)		Loss of HCl	CuO
	120–900		3	71.92 (71.17)	80.51 (80.43)	Loss of 2H <sub>2</sub> O and H <sub>2</sub> L <sup>4</sup>	
[Ni(HL <sup>4</sup> )Cl(H <sub>2</sub> O) <sub>3</sub> ]	30–100	71, 152, 551, 828	1	10.68 (9.09)		Loss of HCl	NiO
	100–900		3	72.33 (72.73)	83.01 (81.82)	Loss of 2H <sub>2</sub> O and H <sub>2</sub> L <sup>4</sup>	

n\* = number of decomposition steps.

range of 25–130 and 30–100 °C corresponds to the loss of one and half and two hydrated water molecules with an estimated mass loss of 6.22% (5.82%) and 7.24% (calcd. 7.45%), for [Cu(HL<sup>1</sup>)Cl(H<sub>2</sub>O)<sub>3</sub>].1.5H<sub>2</sub>O and [Ni(HL<sup>2</sup>)Cl(H<sub>2</sub>O)<sub>3</sub>].2H<sub>2</sub>O chelates, respectively. While the second and third steps of decomposition correspond to the loss of coordinated water molecules and HCl gas within the temperature range of 130–330 and 100–300 °C with an estimated mass loss of 16.35% (15.63) and 18.49% (calcd. 18.72%) for [Cu(HL<sup>1</sup>)Cl(H<sub>2</sub>O)<sub>3</sub>].1.5H<sub>2</sub>O and [Ni(HL<sup>2</sup>)Cl(H<sub>2</sub>O)<sub>3</sub>].2H<sub>2</sub>O chelates, respectively. In the final steps of decomposition within the temperature range of 330–900 and 300–900 °C, estimated mass losses of 61.16% (calcd. 62.21%) and 57.17% (calcd. 58.74%) are observed and can be attributed to the loss L<sup>1</sup> and L<sup>2</sup> ligand molecules leaving CuO and NiO as a residue for [Cu(HL<sup>1</sup>)Cl(H<sub>2</sub>O)<sub>3</sub>].1.5H<sub>2</sub>O and [Ni(HL<sup>2</sup>)Cl(H<sub>2</sub>O)<sub>3</sub>].2H<sub>2</sub>O chelates, respectively.

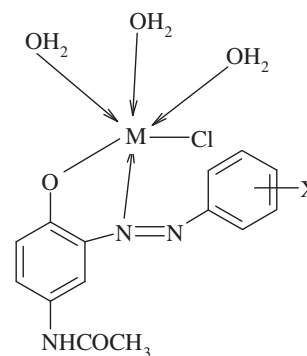
In addition, [Cu(HL<sup>2</sup>)Cl(H<sub>2</sub>O)<sub>3</sub>] and [Ni(HL<sup>3</sup>)Cl(H<sub>2</sub>O)<sub>3</sub>] chelates show five steps of decomposition. The first two steps of decomposition within the temperature range of 30–190 and 30–100 °C correspond to the loss of HCl and two coordinated water molecules and HCl and HBr and two water molecules of coordination with an estimated mass loss of 15.48% (16.04%) and 31.82% (calcd. 31.88%), for [Cu(HL<sup>2</sup>)Cl(H<sub>2</sub>O)<sub>3</sub>] and [Ni(HL<sup>3</sup>)Cl(H<sub>2</sub>O)<sub>3</sub>] chelates, respectively. While the remaining steps of decomposition correspond to the loss of HL<sup>2</sup> and HL<sup>3</sup> ligands within the temperature range of 190–800 and 350–850 °C with an estimated mass loss of 67.81% (calcd. 66.59) and 57.34% (calcd. 57.11%) for [Cu(HL<sup>2</sup>)Cl(H<sub>2</sub>O)<sub>3</sub>] and [Ni(HL<sup>3</sup>)Cl(H<sub>2</sub>O)<sub>3</sub>] chelates, respectively.

On the other hand, in the [Cu(HL<sup>3</sup>)Cl(H<sub>2</sub>O)<sub>3</sub>] complex, the first two steps in the temperature range of 30–250 °C, with an estimated mass loss of 20.98% (calcd. 19.06%) can be

attributed to the loss of HCl gas and three water molecules. The mass losses of the remaining decomposition steps within the temperature range of 250–950 °C correspond to the decomposition of HL<sup>3</sup> ligand leaving CuO as a residue (Table 3).

### 3.4. Structural interpretation

From all of the above observations, the structure of all complexes for four ligands may be interpreted with a similar distribution of like coordinating sites, which coordinated to Cu(II) and Ni(II)



H<sub>2</sub>L<sup>1</sup>; X = OCH<sub>3</sub>  
H<sub>2</sub>L<sup>2</sup>; X = p-NO<sub>2</sub>  
H<sub>2</sub>L<sup>3</sup>; X = p-Br  
H<sub>2</sub>L<sup>4</sup>; X = H

M = Ni(II) and Cu(II).

**Figure 2** Proposed structural formulae of metal complexes.

ions and takes place via the phenolic O and azo N atom. Although ligands do not have the same fragments, they all contain the same coordinating sites, arranged in the same way. Thus, their coordinating behaviour described in the crystal structure of their complexes is relevant for the interpretation of the ligands' coordinating capacity. The structure information from these complexes is in agreement with the data reported in this paper based on the elemental analysis, IR, and electronic spectra measurements. Consequently, the structures proposed are based on octahedral geometry. The proposed general structures are shown in Fig. 2.

#### 4. Biological activity

The  $[\text{Cu}(\text{HL}^1)\text{Cl}(\text{H}_2\text{O})_3]$  complex was the most biologically active compound which caused 18, 50, and 83 of the adult *Tribolium confusum* mortality by the concentration of 10%, 30%, and 50%, respectively. The highest concentration (50) of the different compounds produced 73%, 57%, 37%, 54%, 56%, 16%, and 74% mortalities of adult *T. confusum* by the compounds of  $[\text{Ni}(\text{HL}^1)\text{Cl}(\text{H}_2\text{O})_3]$ ,  $[\text{Ni}(\text{HL}^2)\text{Cl}(\text{H}_2\text{O})_3]$ ,  $[\text{Cu}(\text{HL}^2)\text{Cl}(\text{H}_2\text{O})_3]$ ,  $[\text{Cu}(\text{HL}^3)\text{Cl}(\text{H}_2\text{O})_3]$ ,  $[\text{Ni}(\text{HL}^3)\text{Cl}(\text{H}_2\text{O})_3]$ ,  $[\text{Ni}(\text{HL}^4)\text{Cl}(\text{H}_2\text{O})_3]$ , and  $[\text{Cu}(\text{HL}^4)\text{Cl}(\text{H}_2\text{O})_3]$ , respectively. Similar finding of chemical compound 2-[(5-chloro-2-methoxyphenyl)azo]-1*H*-imidazole (M6434) produced lethal shock of survival rates in hemorrhagic and endotoxin-shock rats at the dose of 3 or 10  $\mu\text{g}/\text{kg}/\text{min}$ . Also, it decreased the blood pressure and the urine output of shocked rabbits (Ohnishi et al., 1984). On the other hand, survival rates of cardiogenic-shock rats improved, and the content of ATP and creatine phosphate in myocardium of these animals was restored by the treatment with 1 or 3  $\mu\text{g}/\text{kg}/\text{min}$  of M6434. On the other hand Chu et al. (2004) reported that, the biodistribution of 11-(1-imidazolyl)-undecanoic acid (IUA) and 11-(2-(4-bromophenylazo)-1-imidazolyl)-undecanoic acid (BPIUA) in mice demonstrated poor heart blood ratios. In addition, these complexes were used for the metabolic myocardial imaging in these animals. Similar results were obtained by US patent (2004). They conducted that the invention relates to novel 6486191. Nitrophenyl-sulphonyl-imidazoles (6486191) is used for the controlling of vegetable and animal pests. In addition the invention of (6486191) has fungicidal properties. Moreover, Lecroise et al. (2008) reported that the synthetic 4-phenylazobenzoyloxycarbonyl-L-leucyl-glycyl-L-prolyl-D-arginine inhibited the metabolism of stoichiometrically collagenase enzyme of *Hypoderma lineatum* insect. Meanwhile the synthetic peptide of *N*-(4-[4'-(dimethylamino)phenylazo]benzoyl-Evyaves-5-[(2-aminoethyl)amino]naphthalene-1-sulfonic acid was a bioactive substrate inhibitor for serralsin-type enzyme of *Photorehabdus luminescens* insect larvae (Marokhazi et al., 2007).

#### 5. Conclusion

The ligands have coordinating sites which are suitably spatially arranged to bind transition metals which require hexa coordination. The similarity of both moieties is outstanding. Work is now underway to assess the validity of these assumptions.

#### References

- Badea, M., Olar, R., Cristurean, E., Marinescu, D., Emandi, A., Budrugaec, P., Segal, E., 2004. Thermal stability study of some azo-derivatives and their complexes, Part 2. New azo-derivative pigments and their Cu(II) complexes. *J. Therm. Anal. Calor.* 77 (3), 815–824.
- Bin, W., Yi-Qun, W., Dong-Hong, G., Fu-Xi, G., 2003. Optical parameters and absorption of azo dye and its metal-substituted compound thin films. *Chin. Phys. Lett.* 20 (9), 1596–1599.
- Chu, T., Zhang, Y., Liu, X., Wang, Y., Hu, S., Wang, X., 2004. Synthesis and biodistribution of  $^{99\text{m}}\text{Tc}$ -carbonyltechnetium-labeled fatty acids. *Appl. Radiat.* 60 (6), 845–850.
- Cotton, F.A., Wilkinson, G., Murillo, C.A., Bochmann, M., 1999. *Advanced Inorganic Chemistry*, sixth ed. Wiley, New York.
- Fu-Xin, H., Yi-Qun, W., Dong-Hong, G., Fu-Xi, G., 2003. Spectroscopy and optical properties of novel metal (II)-azo complex films in blue-violet light region. *Chin. Phys. Lett.* 20, 2259–2261.
- Gan, F.X., Hou, L.S., Wang, G.B., Liu, H.Y., Li, J., 2000. Optical and recording properties of short wavelength optical storage materials. *Mat. Sci. and Eng. B* 76, 63–68.
- Geng, Y., Gu, D., Gan, F., 2004. Application of novel azo metal thin film in optical recording. *Opt. Mater.* 27 (2), 193–197.
- Hamada, E., Fujii, T., Tomizawa, Y., Imura, S., 1997. High Density Optical Recording on Dye Material Discs: An Approach for Achieving 4.7 GB Density. *Jpn. J. Appl. Phys.* 36, 593–594.
- Katz, H.E., Singer, K.D., Sohn, J.E., Dirk, C.W., King, L.A., Gordon, H.M., 1987. Greatly enhanced second-order nonlinear optical susceptibilities in donor-acceptor organic molecules. *J. Am. Chem. Soc.* 109 (21), 6561–6563.
- Koh, J., Greaves, A.J., 2001. Synthesis and application of an alkali-clearable azo disperse dye containing a fluoro-sulfonyl group and analysis of its alkali-hydrolysis kinetics. *Dyes Pigm. (SCI)* 50 (2), 117–126.
- Lecroise, A., Boulard, C., Keil, B., 2008. Chemical and enzymatic characterization of the collagenase from the insect hypoderma lineatum. *J. Eur. Biochem. Societies.* 101 (2), 385–393.
- Li, X.Y., Wu, Y.Q., Gu, D.D., Gan, F.X., 2009. Optical characterization and blu-ray recording properties of metal(II) azo barbituric acid complex films. *Mater. Sci. Eng. B* 158 (1–3), 53–57.
- Li, X., Wu, Y., Gu, D., Gan, F., 2010. Spectral, thermal and optical properties of metal(II)-azo complexes for optical recording media. *Dyes Pigm.* 86 (2), 182–189.
- Marokhazi, J., Mihala, N., Hudecz, F., Fodor, A., Graf, L., Venekei, I., 2007. Cleavage site analysis of a serralsin-like protease, PrtA, from an insect pathogen *Photorehabdus luminescens* and development of a highly sensitive and specific substrate. *FEBS J.* 274 (8), 1946–1956.
- Mohamed, G. G., 1996. Spectrophotometric and potentiometric studies on the chemical behaviour of acetamidophenol drugs during reaction with bromine. Ph.D. Thesis, Cairo University.
- Mohamed, G.G., El-Gamel, N.E.A., Teixidor, F., 2001a. Complexes of 2-(2-benzimidazolylazo)-4-acetamidophenol, a phenoldiazonyl-containing ligand. Could this be a moiety suitable for Zn and Cd extraction. *Polyhedron* 20 (21), 2689–2696.
- Mohamed, G.G., El-Gamel, N.E.A., Nour El-Dien, F.A., 2001b. Preparation, chemical characterization, and electronic spectra of 6-(2-pyridylazo)-3-acetamidophenol and its metal complexes. *Synth. React. Inorg. Met.-Org. Chem.* 31, 347–358.
- Mohamed, G.G., Zayed, M.A., El-Gamel, N.E.A., 2002. Thermal and kinetic studies on solid complexes of 2-(2-benzimidazolylazo)-4-acetamidophenol with some transition metals. *Spectrochim. Acta A* 58 (14), 3167–3178.
- Nejati, K., Rezvani, Z., Seyedahmadian, M., 2009. The synthesis, characterization, thermal and optical properties of copper, nickel, and vanadyl complexes derived from azo dyes. *Dyes Pigm.* 83, 304–311.
- Nishihara, H., 2004. Multi-mode molecular switching properties and functions of azo-conjugated metal complexes. *Bull. Chem. Soc. Jpn.* 77, 407–428.
- Ohnishi, H., Yamaquchi, K., Sato, M., Uemura, A., Funato, H., Dabasaki, T., 1984. Effect of 2-[(5-chloro-2-methoxyphenyl)azo]-1*H*-imidazole (M6434) on hemorrhagic, and endotoxin shock in rats and rabbits. *PMID* 13 (3), 26–70.

- Sabi, Y., Tamada, S., Iwamura, T., Oyamada, M., Bruder, F., Oser, R., Berneth, H., Hassenrück, K., 2003. Development of organic recording media for blue high numerical aperture optical disc system. *Jpn. J. Appl. Phys.* 42, 1056–1058.
- Suzuki, Y., Okamoto, Y., Kurose, Y., Maeda, S., 1999. High-speed Recording Performance of Metal Azo Dye Containing Digital Video Disc-Recordable Discs. *Jpn. J. Appl. Phys.* 38, 1669–1674.
- Wang, S., Shen, S., Xu, H., 2000. Synthesis, spectroscopic and thermal properties of a series of azo metal chelate dyes. *Dyes Pigm.* 44 (3), 195–198.
- Zaki, Z.M., Haggag, S.S., Soayed, A.A., 1998. Studies on Some Schiff Base Complexes of  $\text{Co}^{\text{II}}$ ,  $\text{Ni}^{\text{II}}$  and  $\text{Cu}^{\text{II}}$  Derived from Salicylaldehyde and O-Nitrobenzaldehyde. *Spectrosc. Lett.* 31, 757.
- Zollinger, H., 1961. *Azo and diazo chemistry*. Interscience, New York.
- Zollinger, H., 1987. *Colour chemistry. Syntheses, Properties, and Applications of Organic dyes*. VCH, Weinheim.